

Microstructure, Texture and Property Changes of High Purity Aluminium during Accumulative Roll Bonding and Conventional Rolling

M. Slámová^{1,a}, P. Homola^{1,2,b}, P. Sláma^{1,b}, J. Čížek^{3,c}, I. Procházka^{3,d} and M. Cieslar^{3,e}

¹ VÚK Panenské Břežany, s.r.o., 250 70 Odolena Voda, Czech Republic

² FNSPE, Czech Technical University, Trojanova 13, 12000 Praha 2, Czech Republic

³ Faculty of Math. and Physics, Charles University, Ke Karlovu 3, 12116 Praha 2, Czech Republic

^aslamova.vuk@volny.cz, ^bvuk@volny.cz, ^cjcizek@mbox.troja.mff.cuni.cz,
^divanp@mbox.troja.mff.cuni.cz, ^ecieslar@apollo.karlov.mff.cuni.cz

Keywords: Aluminium, ARB, rolling, microstructure, texture, hardness, positron annihilation.

Abstract. It is known that the severe plastic deformation (SPD) induced by Accumulative Roll Bonding (ARB) results in more important grain refinement as compared to conventional rolling. Since ARB enables production of large amounts of ultra-fine grained (UFG) materials, its adoption into industrial practice is favoured. The paper presents the results of a study of high purity aluminium processed by ARB and cold rolling. Microstructure changes induced by both methods were studied by light and transmission electron microscopy. Dislocation density and arrangement were assessed by positron annihilation spectroscopy. Strength evolution was estimated by hardness measurements. Texture measurements were performed by X-ray diffraction. ARB processing results in over twofold increase in hardness. Hardness increases significantly after two ARB cycles and it raises only a little or decreases during subsequent cycles. The increase in hardness induced by conventional rolling is smaller. Positron lifetime measurements reveal a substantial increase of dislocation density at the first ARB cycle and a moderate increase or even a decrease at further cycles. The high fraction of positrons trapped at grain-boundary dislocations gives evidence for substantial grain refinement confirmed by TEM examinations. Grain size of 1.2 μm in the rolling plane and as small as of 90 nm in the normal direction is obtained. The rolled samples have a typical rolling texture (β -fibre). The β -fibre of the sample ARB processed to strain of 2.4 is weaker as compared to its rolled counterpart and it presents through thickness variations. The surface layers do not have any β -fibre orientations but they have ND-rotated cube texture formed by the shear strains induced by lubricant-free rolling.

Introduction

One of the promising processes of grain refinement by ultra-high plastic deformation is accumulative roll bonding (ARB) [1,2]. ARB does not require any special equipment and in addition, it enables the production of large amounts of ultra-fine grained (UFG) materials. These are the major advantages making ARB suitable for industrial applications. ARB involves multiple repetitions of surface processing, stacking, heating (not mandatory), rolling, and cutting. The rolling bonds the sheets and after 4 to 8 cycles, UFG materials with high strength and relatively good ductility are produced. ARB has been successfully used to prepare UFG sheets from different aluminium alloys [1,2,3], in which the effect of solute atoms and second-phase particles on stabilising UFG structures is of great importance. However, there is only restricted information about the microstructure and properties of ARB processed high purity aluminium [4] and the differences with respect to conventionally rolled sheets. The lack of stabilising solutes and particles in high purity aluminium allows to study the extent of strain recovery that occurs easily even at ambient temperature. The paper presents the results of ARB processing of 4N Al (Al99.99) at ambient temperature. For the sake of comparison, low-speed conventional rolling to strains comparable to ARB induced strains was carried out.

Experimental

The as-provided hot rolled 9.0 mm plate of 4N Al (Al99.99) was cold rolled to thickness of 2.0 mm. Fully recrystallized sheet was prepared by annealing for 30 minutes at 350°C. ARB processing consisted in the repetition of 4 steps: 1) degreasing and wire-brushing with 0.3 mm steel wire brush; 2) stacking of two pieces of 300×50×2 mm³; 3) joining by Al wires; 4) rolling without lubricant to 50% reduction in thickness. Roll diameter of 340 mm and peripheral speed of 0.7 m/min was used. In order to prevent the propagation of edge cracks, specimen edges were trimmed and smoothed down. The 2.0 mm thick sheet was also conventionally cold rolled (CR) at low rate to thickness of 1, 0.5, 0.25 and 0.125 mm, i.e., to the same equivalent strains as obtained by 1 to 4 ARB cycles.

The evolution of sheet microstructure as result of ARB and conventional rolling was studied by light (LM) and transmission electron microscopy (TEM). LM observations were carried out in the long transverse plane (TD-plane) on samples etched in Barker's solution. TEM foils 3 mm in diameter were prepared by twin-jet polishing (-30°C, 30 V) with 6% solution of HClO₄ in methanol. Positron annihilation spectroscopy (PAS), i.e., measurements of positron lifetime (PL) [5], was used for the assessment of dislocation density and arrangement in the input and deformed materials. A positron source ²²Na and a fast-fast PL spectrometer [6] with timing resolution of 160 ps at coincidence count rate 120 s⁻¹ were employed. Microhardness measurements HV0.3 served for the estimation of strength evolution. Texture evaluation by X-ray diffraction was performed at different positions through the thickness of a sample ARB processed by 3 cycles (Fig. 1) and in CR samples. Conventionally rolled samples were analysed after etching to remove a layer of 25 μm. (111), (200) and (220) pole figures were measured and the three-dimensional orientation distribution functions (ODFs) were calculated by the series expansion method [7] with expansion to $l_{\max}=22$.

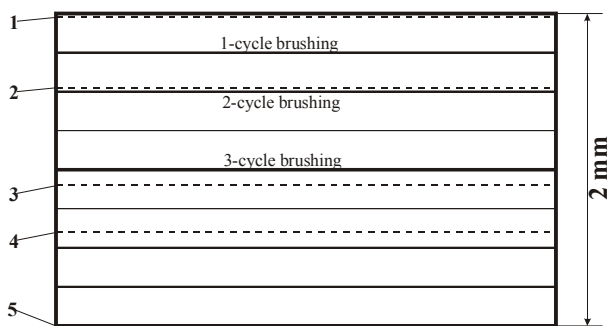


Fig. 1

Positions of texture measurements in sample ARB processed by 3 cycles.

- 1: 25 μm under non-brushed surface;
- 2: 25 μm under surface brushed in 2-cycle
- 3: 100 μm under surface brushed in 3-cycle – near the central plane of initial sheet;
- 4: 100 μm under surface brushed in 2-cycle;
- 5: untreated surface.

Results and Discussion

High purity Al sheets were easily ARB bonded at ambient temperature. Figure 2a shows that the hardness of ARB samples increases from 17.5 to 50, i.e., 2.8 times. Significant hardening occurs during the 1 and 2 cycles, but only a small increase or even a slight softening is observed at subsequent cycles. The increase in hardness produced by the first ARB cycle is larger than this due to conventional rolling to the same equivalent strain ϵ . In subsequent cycles, the hardening rate of both methods is similar.

LM examinations indicated that the initial sheet has fully recrystallized structure with grains of size $l_{RD}=46$ μm and $l_{ND}=38$ μm in the rolling (RD) and normal (ND) directions, respectively (Table 1). TEM observations revealed very low initial dislocation density of 10¹² m⁻².

Grain (subgrain) size of initial and ARB processed Al99.99 [in μm].

initial		1 cycle		2 cycles		3 cycles		4 cycles	
l_{RD}	l_{ND}	$d_{ND-pl.}$	l_{ND}	$d_{ND-pl.}$	l_{ND}	$d_{ND-pl.}$	l_{ND}	$d_{ND-pl.}$	l_{ND}
46	38	2.0	1.3	1.4	0.6	1.2	0.5	1.7	0.5

Table 1

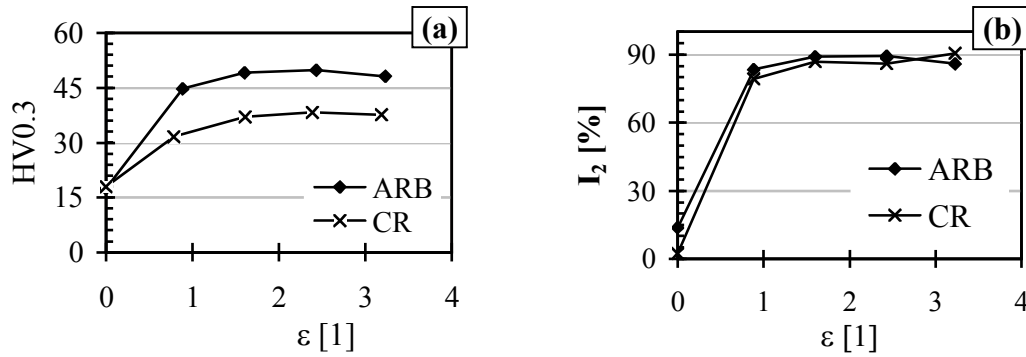


Fig. 2. Variation of microhardness $HV0.3$ (a) and PAS defect intensity component I_2 (b) with strain introduced by ARB processing and cold rolling .

The LM micrographs of ARB samples in Fig. 3 show gradual grain flattening with increasing number of ARB cycles. Slip lines in individual grains and slip bands going through several grains can be distinguished at low strains. Figure 4 shows LM micrographs of CR samples rolled to the same strains as induced by 1 to 4 ARB cycles. The evolution of grain shape in CR samples is practically the same as in ARB samples except for the less pronounced strain localization in shear bands.

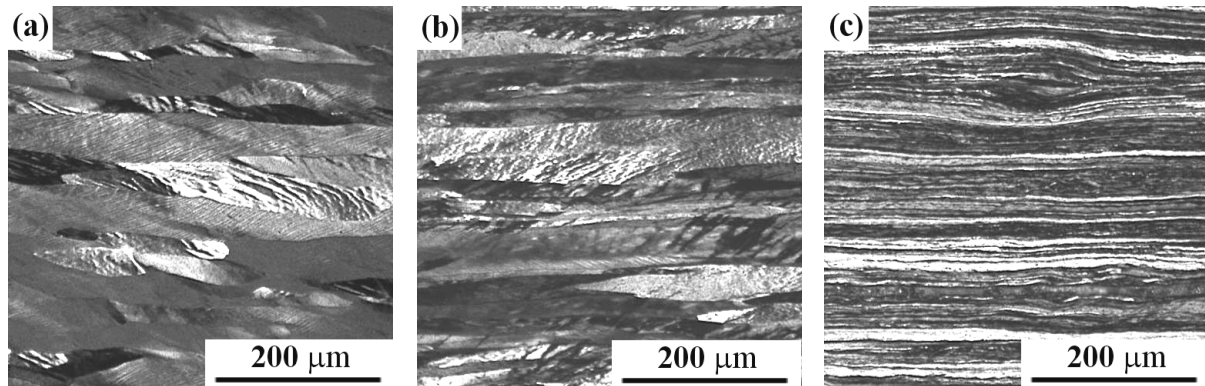


Fig. 3. LM micrographs of ARB samples with strain ϵ of: a) 0.8; b) 1.6; c) 3.2. Observed from TD.

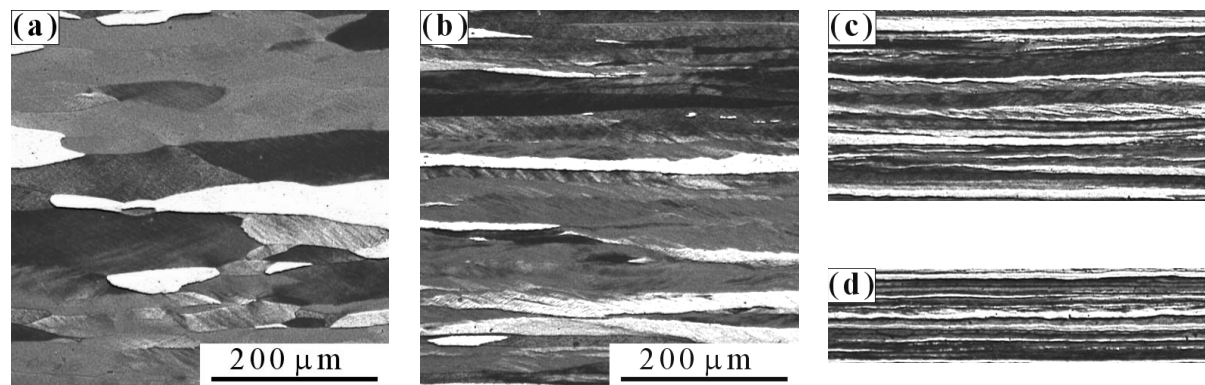


Fig. 4. LM micrographs of sheets cold rolled to equivalent strain ϵ of: a) 0.8; b) 1.6; c) 2.4; d) 3.2. Observed from TD.

The results of PL measurements of ARB processed samples were reported in [10]. It was found out that PL spectra are well fitted by two components: the free positron component with shorter lifetime τ_1 , and a contribution of positrons trapped at defects. The latter component has lifetime of $\tau_2 \approx 243$ ps, which corresponds to dislocations in Al [8]. The relative intensity I_2 of the defect component increases from 15% in the initial sheet to 83% at the first ARB cycle but it changes only moderately during subsequent ARB cycles (Fig. 2b). This is indicative for a substantial increase of defect density during the first ARB cycle, while further cycles do not cause any significant change.

The lifetime τ_2 remains unchanged with increasing strain. This indicates that the nature of defects does not change, i.e., the positrons are in all cases trapped at dislocations. The application of the two-state trapping model [5] to the data reveals that the dislocations are not distributed uniformly, i.e., they are arranged in cell and subgrain boundaries. Fig. 2b shows that the density of dislocations in the CR sample is a little smaller than in the ARB sample.

Figure 5 shows TEM micrographs of ARB processed samples observed from ND (Fig. 5a,b,c) and TD (Fig. 5d,e,f), respectively. In accordance with PL measurements, TEM examinations of the 1st cycle sample show cells and subgrains of size $d_{ND-pl.} = 1-2 \mu\text{m}$ (Fig. 5a) and low dislocation density in their interiors ($3 \cdot 10^{13} \text{ m}^{-2}$). Subgrain formation due to dynamic dislocation recovery does not occur during the 1st cycle but it becomes more intensive with increasing number of ARB cycles. The increased rate of grain refinement is better evidenced by observation from TD (Fig. 5d,e,f). The grains are equiaxed in the rolling plane but they are lamellar when observed from TD. This result does not agree with the nearly equiaxed grains observed by Tsuji et al. [2] in 4N Al ARB processed by 6 cycles. The probable reason for this discrepancy is the different rolling speed used resulting in different sample heating. Heating of up to 200°C is reported in [2] contrarily to our rolling experiments carried out at low rate with heating of less than 60°C. Equiaxed grains were observed from TD only after the 1st cycle. In accordance with the results of PL measurements (Fig. 2b), the density of dislocations in subgrain interiors, also when observed from TD, increases up to the 2nd cycle but it decreases during the 4th cycle.

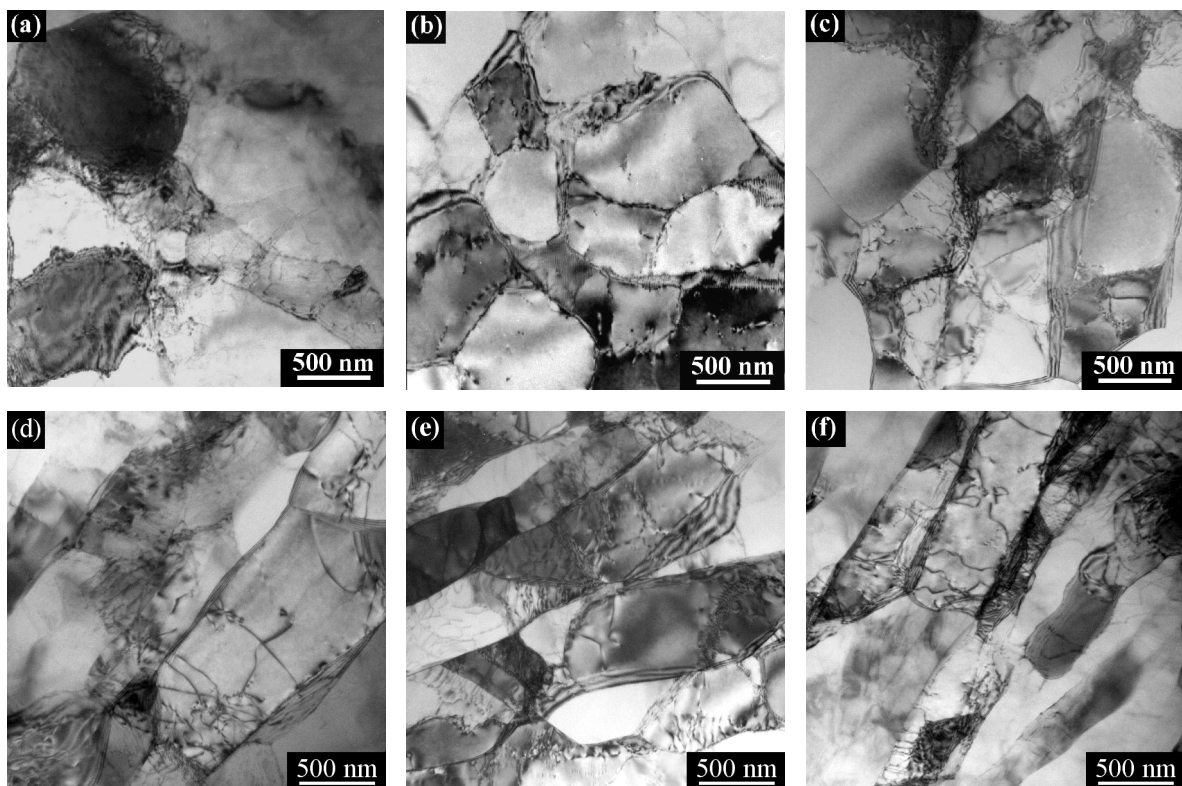


Fig. 5. TEM micrographs of ARB processed samples observed from ND: a) 1 cycle; b) 3 cycles; c) 4 cycles; and from TD: d) 2 cycles, e) 3 cycles, f) 4 cycles.

Assuming that no new high angle boundaries (HAGB) form during both ARB and CR, the mean grain size in samples with strain $\varepsilon = 2.8$ and 3.2 calculated from the initial ND grain size (Table 1) should be of 4.8 and 2.4 μm , respectively. However, much smaller distance between grain boundaries was observed in ND. It is now established that deformation induced grain boundaries (incidental dislocation boundaries – IDB and geometrically necessary boundaries – GNB) form in deformed crystals and they subdivide the initial grains [9]. TEM examinations of our samples thus indicate that initial grains are subdivided by GNB in ND and low angle IDB in RD. High angle

boundaries are observed also in ND and their fraction increases with increasing number of cycles. The grain size is much smaller in ND than in RD and TD. The mean grain size decreases from 1.3 μm in the 1st cycle to 500 nm in the 4th cycle sample (Table 1). Moreover, regions with much finer grains (90 to 160 nm in ND) were found in samples ARB processed by 2 to 4 cycles.

It was thus observed that the boundary spacing decreases and GNB misorientation increases as ARB strain increases. In high purity materials such as 4N Al, the motion of dislocations and grain boundaries is not pinned by second phase particles and easy recovery is expected. However, due to the introduction of friction deformation by the surface brushing preceding the rolling step, additional grain refinement is introduced by ARB processing [2]. This additional grain refinement, which progressively comes into sheet interior, results in more intensive grain refinement in ARB samples as compared to their CR counterparts and is one of the probable causes of the higher work hardening of ARB samples. The redundant shear deformation caused by the friction between rolls and sheet surface (lubricant-free condition) is supposed to be of similar magnitude in both ARB and CR samples. However, the shear deformation is concentrated in the surface layers of CR samples, whereas it enters sheet interior during ARB. Deformation recovery is easy in 4N Al, thus surface shear deformation probably recovers with increasing reduction of conventional rolling, as it does not change its position. In ARB processed samples, the layers deformed in shear come to sheet centre during the next cycle, thus deformation mode changes and makes the recovery less probable. This mechanism could be also responsible for the higher work hardening induced by ARB.

The ODFs measured at several positions of the ARB sample processed by 3 cycles and of its CR counterpart and the corresponding intensities of some texture components are in Fig. 6 and Table 2.

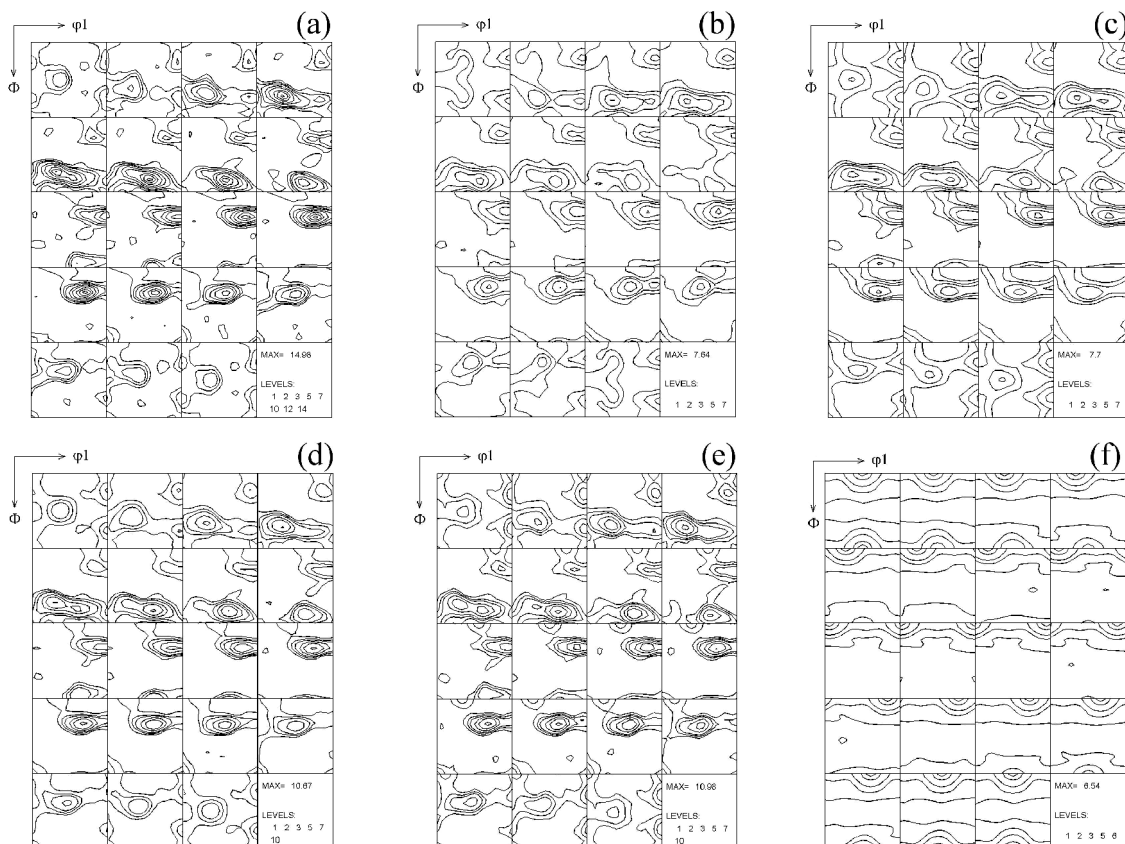


Fig. 6. ODFs of CR (a) and ARB sample at positions (see Fig. 1): 1 (b), 2 (c), 3 (d), 4 (e) and 5 (f). Both samples were deformed to the same strain $\varepsilon = 2.4$.

All conventionally rolled samples (Fig. 6a) and positions 2, 3 and 4 inside the ARB sample present typical rolling texture with β -fibre components and retained cube, cube_{RD} rotated and G orientations. The β -fibre in the ARB sample is fairly weaker than in the conventionally rolled sample. The texture

at 25 μm under the surface of the ARB sample is untypical; it does not contain any Brass orientations. Moreover, pure shear texture $\{001\}\langle 110\rangle$ is observed at its untreated surface. This texture is attributed to the shear deformation induced by the high friction condition of the lubricant-free rolling applied. Texture measurements thus indicate that ARB processing produces samples with weaker texture as compared to conventionally rolled samples.

Maximum intensities of the most important texture components.

Sample	$\{001\}\langle 100\rangle$	$\{013\}\langle 100\rangle$	$\{001\}\langle 310\rangle$	$\{001\}\langle 110\rangle$	$\{011\}\langle 100\rangle$	$\{011\}\langle 110\rangle$	β -fibre
ARB-1	1.7	1.2	1.6	0.7	2.8	0.4	7.4
ARB-2	2.6	2.6	0.7	0.8	2.0	0.8	7.6
ARB-3	1.9	2.1	0.4	0.2	0.5	0.6	10.7
ARB-4	2.5	1.7	0.4	0.2	2.2	0.6	10.9
ARB-5	2.9	1.4	2.8	6.5	0.9	0.7	-
CR	1.3	2.7	1.2	-	1.8	-	15.0

Table 2

Summary

High purity aluminium was processed by ARB and cold rolling. ARB induces more than twofold increase in hardness during the first cycles and saturates in subsequent cycles. Hardness increase due to conventional rolling is smaller. Positron lifetime measurement reveals increase in dislocation density at 1st ARB cycle and moderate increase or decrease at further cycles. PAS gives evidence for substantial grain refinement confirmed by TEM examinations. Grain size of 1.2 μm in ND-plane and as small as 90 nm in ND is obtained. The conventionally rolled samples present stronger rolling texture than the interior of ARB sample, which texture presents through thickness variations. The surface of the ARB sample has a ND-rotated cube texture due to lubricant-free rolling conditions.

Acknowledgments: The financial support of the Ministry of Education, Youth and Sports of the Czech Republics under projects No. MSM2631691901 and GACR (106/05/0073) are gratefully acknowledged. AL INVEST Břidličná, a.s. is acknowledged for supplying the experimental material.

References

- [1] N. Tsuji, N. Kamikawa, H.W. Kim and Y. Minamino: Ultrafine Grained Materials III (TMS, OH, 2004), p. 219.
- [2] N. Tsuji, X. Huang and H. Nakashima: Evolution of Deformation Microstructure in 3D (Riso National Laboratory, Denmark 2004), p. 147.
- [3] M. Karlík, P. Homola and M. Slámová: J. of Alloys and Compounds 378 (2004), p. 322.
- [4] Y. Koizumi, Y. Saito, N. Tsuji, Y. Minamino and K. Ota, J. Alloys Comp. 355 (2003), p. 47.
- [5] P. Hautojärvi and C. Corbel: Positron Solid State Physics, Eds. A. Dupasquier and A.P. Mills (IOS Press, Varena 1995), p. 491.
- [6] F. Bečvář, J. Čížek, L. Lešták, I. Novotný, I. Procházka and F. Šebesta: Nucl. Instr. Meth. A. 443 (2000), p. 557.
- [7] Bunge H. J., Mathematical Methods of Texture Analysis (Butterworths, London 1984).
- [8] J. Čížek, I. Procházka, T. Kmječ and P. Vostrý: phys. stat. sol. (a) 180 (2000), p. 439.
- [9] N. Hansen: Metall. Mater. Trans. 32A (2001), p. 2917.
- [10] Slámová M., Homola P., Karlík M., Čížek J., Procházka I. and Cieslar M.: Evolution of Deformation Microstructure in 3D (Riso National Laboratory, Denmark 2004), p. 521.